THE ASTROPHYSICAL JOURNAL, 492:415–419, 1998 January 1

EFFECTIVE COLLISION STRENGTHS FOR FINE-STRUCTURE TRANSITIONS FROM THE $3s^2 3p^5\ ^2P$ GROUND STATE OF CHLORINE–LIKE Ni XII

A. MATTHEWS,[1] C. A. RAMSBOTTOM,[2] K. L. BELL,[2] AND F. P. KEENAN[1]

Received 1997 May 19; accepted 1997 August 13

ABSTRACT

The *R*-matrix method is used to compute electron impact collision strengths for transitions in Ni XII from its ground-state fine-structure levels. Sophisticated configuration-interaction wave functions are used to represent the 14 lowest *LS* target states employed in the *R*-matrix expansion. By transforming the *LS*-coupled reactance matrices, and by assuming a Maxwellian velocity distribution for the incident electrons, the effective collision strengths are calculated for the $3s^2 3p^5\ ^2P^o_{1/2}$–$3s^2 3p^5\ ^2P^o_{3/2}$ transition within the ground state and from both these fine-structure levels to the 29 excited levels arising from states obtained from $3s3p^6$ and $3s^2 3p^4 3d$ configurations. Effective collision strengths, obtained in the temperature range log T_e = 3.2–6.6 (K), are expected to have an accuracy of better than 20%.

Subject headings: atomic data — atomic processes

1. INTRODUCTION

Emission lines from ions of iron have been frequently detected in the EUV solar spectrum, and they provide some of the most useful electron density diagnostics currently available (Brickhouse, Raymond, & Smith 1995). However, this is not the case at present for ions of nickel, for which only a small number of emission lines, from Ni XV to Ni XVII, have been observed, and even these are only weakly detected (Dere et al. 1979).

The Coronal Diagnostic Spectrometer (CDS) instrument on board SOHO, with its ability to obtain high–spectral resolution and high–signal-to-noise observations, presents an ideal opportunity to measure reliable emission-line strengths for weak nickel features in the solar EUV spectrum (Harrison et al. 1995). Many Ni XII emission lines lie in the 152–317 Å wavelength range, which is covered by CDS. Such measurements will necessitate comparison with theoretical emission-line intensities calculated using atomic data, in order to investigate the usefulness of Ni XII line ratios as electron density and/or temperature diagnostics for the solar transition region.

There are also extensive Ni XII spectra from the Joint European Torus (JET) tokamak, for which the plasma parameters (electron temperature and density) have been independently determined. The JET observations will therefore provide a very powerful test of the Ni XII diagnostic calculations. In addition, the JET spectra contain primarily emission lines from ions of nickel, while the CDS observations will consist of features from many elements present in the solar atmosphere, and from iron in particular. A comparison of the two will allow the extent of blending in the CDS data to be properly assessed.

Apart from the calculation by Pelan & Berrington (1995) for the transition between the fine-structure levels of the ground state, the authors are unaware of any other existing theoretical or experimental atomic collision data for Ni XII required for a reliable calculation of emission-line ratios. We therefore believe our paper to be the first to present not only results, but accurate data for the appropriate effective collision strengths.

The present calculation uses the *R*-matrix method (Burke & Robb 1975) and includes the 14 lowest lying *LS* target states: $3s^2 3p^5\ ^2P^o$; $3s3p^6\ ^2S$; $3s^2 3p^4(^3P)3d\ ^4D, ^4F, ^4P, ^2F, ^2P, ^2D$; $3s^2 3p^4(^1D)3d\ ^2P, ^2D, ^2G, ^2F, ^2S$; and $3s^2 3p^4(^1S)3d\ ^2D$. The wave function for each of these target states was determined by using the code CIV3 (Hibbert 1975) and so is expressed in configuration-interaction form. The *LS* coupling reactance matrices obtained from the *R*-matrix calculation were transformed using a unitary transformation (Saraph 1978) in order to calculate the fine-structure collision strengths. Effective collision strengths were then determined by averaging the collision strengths over a Maxwellian distribution of electron velocities.

2. CALCULATION DETAILS

2.1. *Target Wave Functions*

The configuration-interaction code CIV3 was used to calculate the wave functions and energy levels of Ni XII in *LS* coupling. Each term was represented by wave functions of the form

$$\Psi(LS) = \sum_{i=1}^{M} a_i \Phi_i(\alpha_i LS)\ , \qquad (1)$$

where each of the configurational wave functions $\{\Phi\}$ is built from one-electron functions (orbitals), whose angular momenta are coupled in a manner defined by $\{\alpha_i\}$, to form a total *L* and *S* common to all configurations in equation (1). The mixing coefficients $\{a_i\}$ are determined variationally (Hibbert 1975).

The one-electron radial functions are represented by a linear combination of Slater-type orbitals:

$$P_{nl}(r) = \sum_{j=1}^{k} C_{jnl}\, r^{I_{jnl}} \exp\,(-\xi_{jnl}\, r)\ , \qquad (2)$$

and the parameters, C_{jnl}, I_{jnl}, and ξ_{jnl} are also determined variationally (Hibbert 1975).

Ten orthogonal orbitals were used in the calculation, six "spectroscopic" orbitals (1*s*, 2*s*, 2*p*, 3*s*, 3*p*, 3*d*) and four pseudo-orbitals ($\overline{4}s$, $\overline{4}p$, $\overline{4}d$, $\overline{4}f$), the latter being included to allow for additional correlations. The *R*-matrix code requires each target state to be represented in terms of a single orbital basis, so the choice of orbital parameters was

[1] Department of Pure and Applied Physics, Queen's University of Belfast, Belfast BT7 1NN, Northern Ireland.

[2] Department of Applied Mathematics and Theoretical Physics, Queen's University of Belfast, Belfast BT7 1NN, Northern Ireland; A.Matthews@qub.ac.uk.

determined as follows. The 1*s*, 2*s*, 2*p*, 3*s*, and 3*p* orbitals were taken to be the Hartree-Fock functions for the ground $3s^2 3p^5\ ^2P^o$ state of Ni XII (Clementi & Roetti 1974). The 3*d* spectroscopic orbital was optimized on the energy of the $3s^2 3p^4(^3P)3d\ ^4D$ state, using the $3s^2 3p^4(^3P)3d$ configuration; considerable care was taken in the selection of state for the energy optimization, and also with the parameter optimization, so that the orbital was a true spectroscopic orbital and not "contaminated" by a correlation orbital component. The correlating pseudo-orbitals ($\overline{4s}$, $\overline{4p}$, $\overline{4d}$, $\overline{4f}$) were optimized as follows: the $\overline{4s}$ orbital was optimized on the energy of the $3s3p^6\ ^2S$ state of Ni XII, using the configurations $3s3p^6$, $3s^2 3p^4(^1D)3d$, and $3s3p^6\overline{4s}$, and was included in order to make an allowance for the different 3*s* orbitals arising in the different states. The $\overline{4p}$ orbital was optimized on the energy of the $3s^2 3p^4(^1S)3d\ ^2D$ state, using the configurations $3s^2 3p^4(^3P, ^1S)3d$, $3s^2 3p^3 3d\overline{4p}$ and allows for correction to 3*p* orbitals. The $\overline{4d}$ orbital was optimized on the energy of the $3s^2 3p^4(^1D)3d\ ^2S$ state, using the configurations $3s3p^6$, $3s^2 3p^4(^1D)3d$, and $3s^2 3p^4(^1D)\overline{4d}$ and is included to account for the strong coupling between $3s3p^6$ and $3s^2 3p^4$ levels. The $\overline{4f}$ orbital was optimized on the energy of the $3s^2 3p^4(^3P)3d\ ^2P$ state, using the configurations $3s^2 3p^4(^1D, ^3P)3d$, and $3s^2 3p^3 3d\overline{4f}$. In the above description of the orbital optimization, it has been implicit that the 1*s*, 2*s*, and 2*p* shells remain closed.

All 14 *LS* eigenstates were represented as a linear combination of all possible configurations arising from one electron replacement from the above orbital set in the two basis configurations, $3s^2 3p^4 3d$ and $3s3p^6$, the 1*s*, 2*s*, and 2*p* shells remaining closed. A total of 481 configurations were therefore required to represent the target states. In Table 1 we compare the energies obtained in this work with theoretical energies (averaged over *J*-values) calculated by Fawcett (1987). We note that Fritzsche et al. (1995) have also computed energy data but have not considered all levels included in this paper. Agreement between the present work and the values of Fawcett is satisfactory, the greatest differences occuring for the $3s^2 3p^5\ ^2P^o$–$3s^2 3p^4(^1D)3d\ ^2S$, $3s^2 3p^4(^3P)3d\ ^2P$, and $3s^2 3p^4(^3P)3d\ ^2D$ separations.

2.2. *The Continuum Expansion*

The total wave function describing the collision is expanded in the *R*-matrix internal region ($r < a$) in terms of the following basis (Burke & Robb 1975; Berrington et al. 1978, 1987):

$$\Psi_k = A \sum_{ij} C_{ijk}\, \overline{\Phi}_i(x_1, x_2 \ldots, x_N, r_{N+1}\, \sigma_{N+1}) u_{ij}(r_{N+1}) + \sum_j d_{jk}\, \phi_j(x_1, x_2 \ldots, x_{N+1}) \,. \quad (3)$$

A is the antisymmetrization operator that ensures that the total wave function satisfies the Pauli exclusion principle. The $\overline{\Phi}_i$ are channel functions formed by coupling the target states to the angular and spin function of the scattered electron. The u_{ij} are the continuum basis orbitals representing the scattered electron, and the ϕ_j are $(N+1)$-electron bound configurations formed from the atomic orbital basis, included to ensure completeness of the total wave function and to allow for short-range correlation.

The continuum orbitals u_{ij} are solutions of the radial differential equation

$$\left[\frac{d^2}{dr^2} - \frac{l_i(l_i+1)}{r^2} + V(r) + k_i^2\right] u_{ij}(r) = \sum_k \lambda_{ijk} P_k(r) \,, \quad (4)$$

which satisfies the boundary conditions

$$u_{ij}(0) = 0 \quad (5)$$

and

$$\frac{a}{u_{ij}} \frac{du_{ij}}{dr}\bigg|_{r=a} = b \,. \quad (6)$$

In equation (4), l_i is the angular momentum of the scattered electron, and $V(r)$ is the static potential of the target in its ground state. The λ_{ijk} are Lagrange multipliers, obtained by imposing the orthogonality of the continuum orbitals to the bound radial orbitals with the same value of l_i.

Twenty continuum orbitals were included for each channel angular momentum to ensure convergence in the energy range considered (0–121 ryd). A zero logarithmic derivative ($b = 0$) was imposed on these continuum orbitals at an *R*-matrix boundary radius of $a = 4.8$ au.

The coefficients C_{ijk} and d_{jk} in equation (3) were found by diagonalizing the $(N+1)$-electron nonrelativistic Hamiltonian within the inner region. The *R*-matrix is then calculated on the boundary between the inner and outer regions.

Long-range coupling between channels is important in the outer region, and the coupled radial differential equations for $r > a$ are solved using a perturbation technique. This obtains the reactance *K*-matrices by matching solutions in the inner and outer regions ($r = a$). Collision strengths are then found.

In the current 14-state *R*-matrix calculation, all partial waves with $L \leq 12$ for both even and odd parities and spin multiplicities (doublets and quartets) are considered. While these are sufficient to permit convergence of the collision strength for the forbidden transitions, it is necessary for dipole-allowed transitions to include higher partial waves with $L > 12$. It is assumed that the high-L behavior of partial collision strengths for these transitions may be represented by a geometrical series with a geometric scaling factor equal to the ratio of two adjacent terms. The justification for this procedure has been given in earlier work by Ramsbottom et al. (1994), Ramsbottom, Berrington, & Bell (1995), and Ramsbottom, Bell, & Stafford (1996).

TABLE 1

TARGET STATE ENERGIES RELATIVE TO THE $3s^2 3p^5\ ^2P^o$ GROUND STATE OF Ni XII COMPARED TO THE CALCULATED VALUES OF FAWCETT (1987)

State	Fawcett (ryd)	Present (ryd)
$3s^2 3p^5\ ^2P^o$	0.000000	0.000000
$3s3p^6\ ^2S$	3.013910	2.910577
$3p^4(^3P)3d\ ^4D$	4.046062	4.121532
$3p^4(^1D)3d\ ^2P$	4.443840	4.477151
$3p^4(^3P)3d\ ^4F$	4.386846	4.477935
$3p^4(^3P)3d\ ^4P$	4.577336	4.613525
$3p^4(^1D)3d\ ^2D$	4.581694	4.630156
$3p^4(^3P)3d\ ^2F$	4.644250	4.721190
$3p^4(^1D)3d\ ^2G$	4.702100	4.760919
$3p^4(^1D)3d\ ^2F$	5.038180	5.095352
$3p^4(^1S)3d\ ^2D$	5.411798	5.476525
$3p^4(^1D)3d\ ^2S$	5.603740	5.749410
$3p^4(^3P)3d\ ^2P$	5.866190	6.139246
$3p^4(^3P)3d\ ^2D$	5.999256	6.252753

It is noted that the collision strengths determined by the *R*-matrix computer packages are for *LS* states only. The fine-structure collision strengths are found by transforming to a *jj*-coupling scheme by utilizing the program of Saraph (1978), which neglects term coupling. The "top-up" from the higher partial waves is again obtained using the geometric series procedure described previously.

In running the *R*-matrix codes, it is customary to adjust the target energy levels to accurate theoretical or experimental values. This ensures that the thresholds are in the correct places, and it also improves the positions of resonances. In this work we therefore adjusted the levels to those given by Fawcett (1987). Any such adjustment must not, however, alter the order of the levels, and we note that the present work finds the $3s^2 3p^4(^3P)3d\ ^4F$ and $3s^2 3p^4(^1D)3d\ ^2P$ states to be almost degenerate and to be in the reverse order of that found by Fawcett (see Table 1). We therefore followed the customary procedure and made these two states degenerate, with a common value of the energy corresponding to that found by Fawcett for the $3s^2 3p^4(^1D)3d\ ^2P$ state. It should also be noted that the value found by Fawcett for the energy of the $3s3p^6\ ^2S$ state has recently been supported by the experimental result of 3.01414 ryd obtained by Träbert (1993).

Finally, it is important for astrophysical and plasma applications to know the effective collision strengths γ_{if} or the excitation-rate coefficients q_{if} (Eissner & Seaton 1974). These are found by averaging the electron collision strengths (Ω_{if}) over a Maxwellian distribution of electron velocities:

$$\gamma_{if}(T_e) = \int_0^\infty \Omega_{if}(E_f) \exp(-E_f/kT) d(E_f/kT) , \qquad (7)$$

and

$$q_{if} = \frac{8.63 \times 10^{-6}}{\omega_i T_e^{1/2}} \gamma_{if}(T_e) \exp(-\Delta E/kT_e) \text{ cm}^3 \text{ s}^{-1} , \qquad (8)$$

where Ω_{if} is the collision strength between fine-structure levels i and f, E_f is the kinetic energy of the final electron, T_e is the electron temperature (K), k is Boltzmann's constant, ω_i is the statistical weight of the lower state, and ΔE is the energy difference (ryd) between the upper and lower states.

3. RESULTS AND DISCUSSION

Using the previously described approximation, we have calculated cross sections for electron collisional excitation of Ni XII. A fine energy mesh of less than 0.005 ryd was used to resolve the resonance structure for the range of impact energies 0–121 ryd. This impact energy range was sufficient for the Maxwellian averaging employed to derive effective collision strengths at the electron temperatures of interest, while the fine mesh was necessary for allowing the resonance structure in the collision cross sections to be properly resolved for each transition. Resonances found below the highest excitation threshold included [i.e., $3p^4(^3P)3d\ ^2D$] are considered to be true resonances, whereas those above this energy level are pseudoresonances arising because of our inclusion of pseudo-orbitals in the wave function representation (Burke, Sukumar, & Berrington 1981). The pseudoresonances are typically found to lie in a restricted energy range—electron energy up to 20 ryd above the final threshold—and, because the higher energy region becomes more important as the temperature increases, it was necessary to average over these pseudoresonances. The background to the total collision strength was extracted from the "raw" data.

We do not propose to tabulate the effective collision strengths obtained in this work for all 59 fine-structure transitions from the two ground-state $3s^2 3p^5\ ^2P^o_{1/2}$ and $^2P^o_{3/2}$ levels to higher fine-structure levels in the temperature range log T_e = 3.2–6.6 K. They can be obtained in electronic form from the author (A.Matthews@Queens-Belfast.AC.UK).

Therefore, in Figures 1–3, we present some of the transitions of interest. The collision strengths are given as a function of incident electron energy in rydbergs, and the effective collision strengths are given as a function of log temperature. The transitions are the following:

1. $3p^5\ ^2P^o_{1/2}$–$3p^5\ ^2P^o_{3/2}$ (Fig. 1). This is an example of a forbidden transition between the fine-structure levels of the $3p^5\ ^2P^o$ ground state in Ni XII. The collision strength presented in Figure 1*a* clearly shows the necessity of including many target states in the wave function, in that a wealth of resonance structure is found to be converging to these thresholds across the entire energy region considered. The fine mesh of energies adopted in the present calculation has clearly ensured that these resonances have been properly resolved. The effect of this structure on the effective collision strength is seen in Figure 1*b*, where the higher lying resonances cause a significant peak to occur at a temperature of about log T_e = 5.5 K. Such enhancements of the effective collision strength for forbidden transitions have been previously found by Ramsbottom et al. (1994, 1995, 1996) when investigating electron impact excitation of N IV, Ne VII, and S II. The results of Pelan & Berrington (1995) for the effective collision strength for the temperature range log T_e = 5.0–7.0 K lie about a factor of 0.55 below the present values. This is due to the several ways in which the present calculation improves upon that of Pelan & Berrington, namely, with a proper account of the *d*-correlation, considerably more sophisticated configuration-interaction wave functions, and adjustment of the energy thresholds to "experimental" values.

2. $3p^5\ ^2P^o_{1/2}$–$3p^4(^3P)3d\ ^4D^e_{5/2}$ (Fig. 2). This is an example of a typical spin-forbidden transition. At low energies the collision strength is significantly enhanced by resonances, whereas the resonance structure at the higher thresholds is relatively insignificant. Thus, in coupling the resonance phenomena with the almost constant collision-strength background, one obtains the typical behavior of effective collision strength versus temperature, with a large peak at the lower temperatures and a rapid decrease as the temperature increases.

3. $3s^2 3p^5\ ^2P^o_{3/2}$–$3s3p^6\ ^2S^e_{1/2}$ (Fig. 3). This is an example of an allowed transition with no change in the principal quantum number, i.e., only a promotion from the 3*s* to the 3*p* orbital. Resonances located at the low energies in this collision strength cause a slight enhancement of the effective collision strength in the low-temperature region. For log $T_e > 5.5$ K, however, the effect of including partial waves $L > 12$ causes the effective collision strength to increase significantly as the temperature increases. Such a behavior is typical for an allowed transition of this kind.

All effective collision strengths have been calculated in the temperature range log T_e = 3.2–6.6, which is sufficient

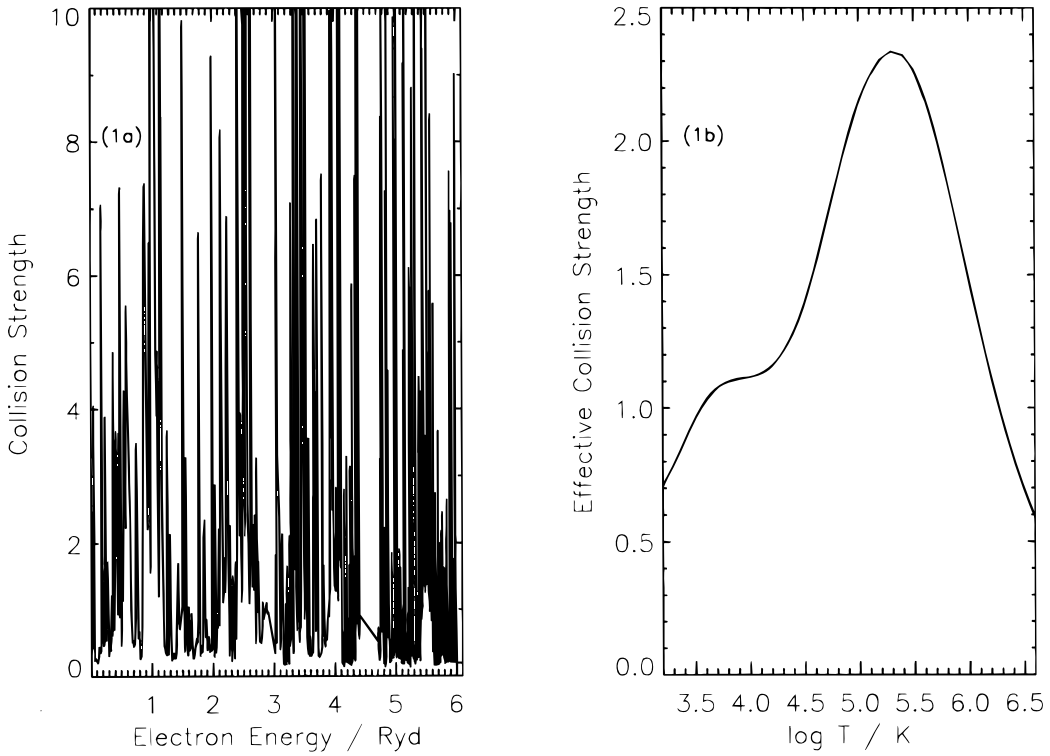

FIG. 1.—(*a*) Collision strength as a function of incident electron energy (ryd), and (*b*) effective collision strength as a function of log T, where T is the electron temperature (K), for the fine-structure transition $3p^5\ ^2P^o_{1/2}$–$3p^5\ ^2P^o_{3/2}$.

for astrophysical applications and diagnostics. The accuracy of our results is difficult to assess. Indeed, the accuracy may be properly assessed only by comparison with experiment or a more sophisticated calculation. Such a calculation will necessitate the availability of more accurate experimental energy levels for the target states and should include relativistic effects "correctly," via the Hamiltonian (noting that the present calculation neglects term coupling

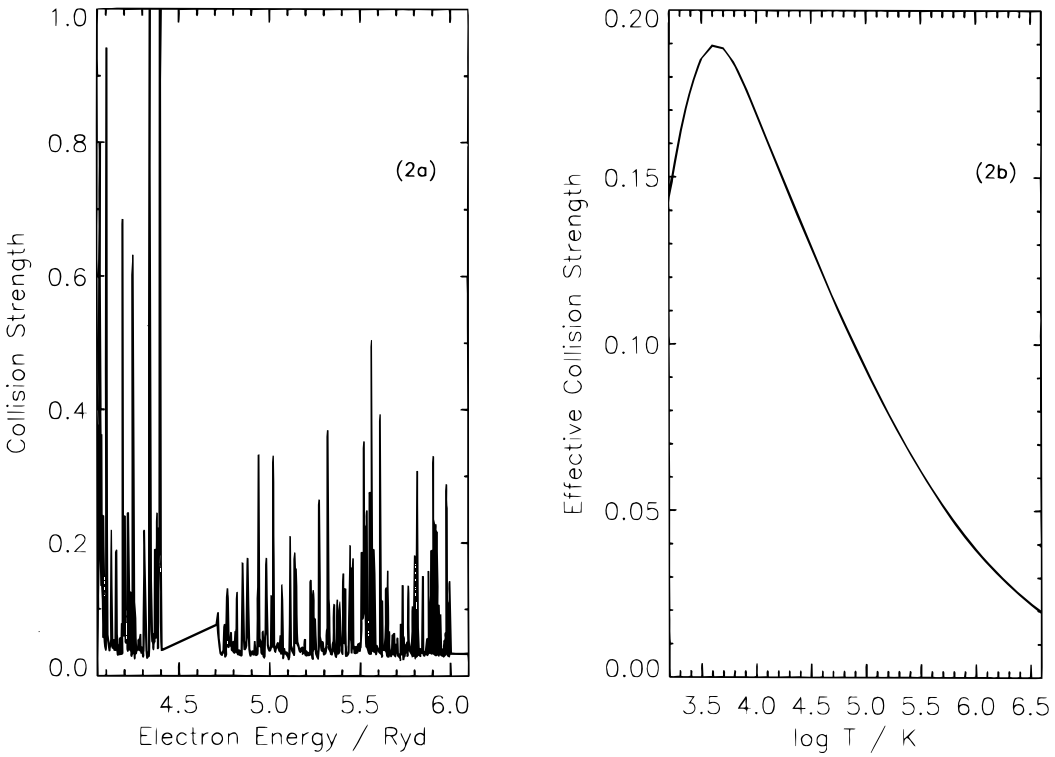

FIG. 2.—(*a*) Collision strength as a function of incident electron energy (ryd), and (*b*) effective collision strength as a function of log T, where T is the electron temperature (K), for the fine-structure transition $3p^5\ ^2P^o_{1/2}$–$3p^4(^3P)3d\ ^4D^e_{5/2}$.

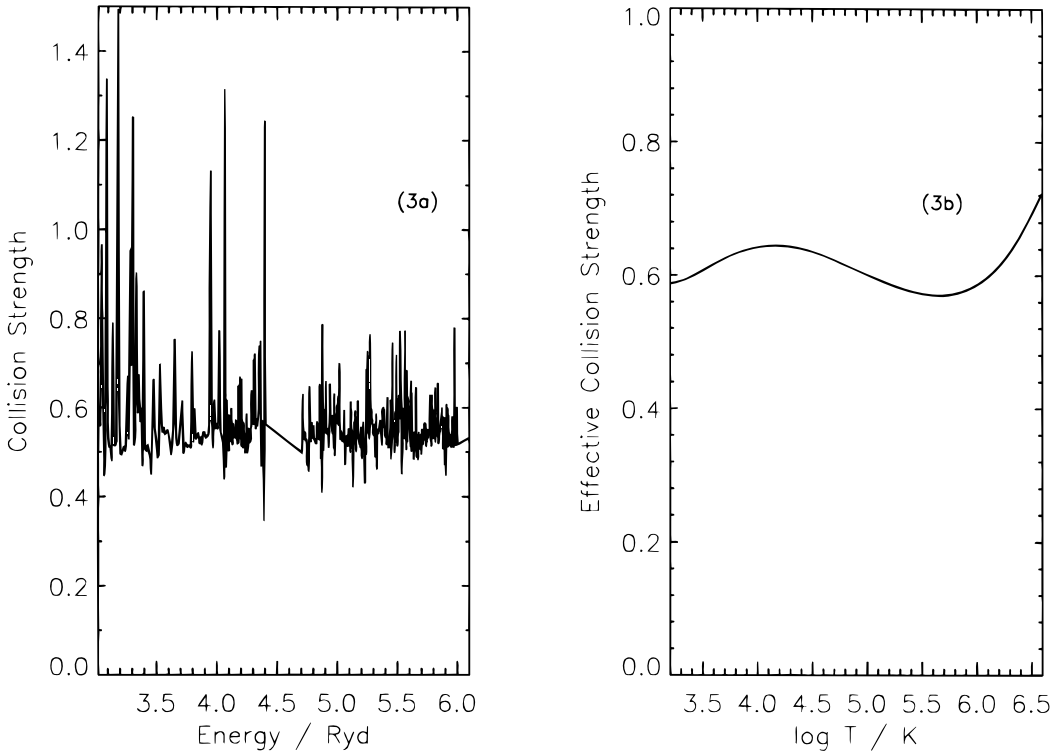

FIG. 3.—(*a*) Collision strength as a function of incident electron energy (ryd), and (*b*) effective collision strength as a function of log T, where T is the electron temperature (K), for the fine structure transition $3p^5\ ^2P^o_{3/2}$–$3s3p^6\ ^2S^e_{1/2}$.

in the intermediate coupling scheme). Alternatively, assessment is possible via the level of agreement between theoretical emission-line ratios derived using the atomic data and those measured for an astrophysical or laboratory plasma. However, from past experience, and noting that the present 14-state *R*-matrix calculation is based on sophisticated configuration-interaction target-state wave functions and that the resonance structure has been fully taken into account, we expect the effective collision strengths to be accurate to better than 20%.

The work reported in this paper has been supported by PPARC, under the auspices of a Rolling Grant, and the computations were carried out on the CRAY J932-SN9522 at Rutherford Appleton Laboratory.

REFERENCES

Berrington, K. A., Burke, P. G., Butler, K., Seaton, M. J., Storey, P. J., Taylor, K. T., & Yu Yan. 1987, J. Phys. B, 20, 6379
Berrington, K. A., Burke, P. G., Le Dourneuf, M., Robb, W. D., Taylor, K. T., & Vo Ky Lan. 1978, Comput. Phys. Commun., 14, 367
Brickhouse, N. S., Raymond, J. C., & Smith, B. W. 1995, ApJS, 97, 551
Burke, P. G., & Robb, W. D. 1975, Adv. At. Mol. Phys., 11, 143
Burke, P. G., Sukumar, C. V., & Berrington, K. A. 1981, J. Phys. B, 14, 289
Clementi, E., & Roetti, C. 1974, At. Data Nucl. Data Tables, 14, 397
Dere, K. P., Mason, H. E., Widing, K. G., & Bhatia, A. K. 1979, ApJS, 40, 341
Eissner, W., & Seaton, M. J. 1974, J. Phys. B, 7, 2533
Fawcett, B. C. 1987, At. Data Nucl. Data Tables, 36, 151
Fritzsche, S., Finkbeiner, M., Fricke, B., & Sepp, W.-D. 1995, Phys. Scr., 52, 258
Harrison, R. A., et al. 1995, Sol. Phys., 162, 233
Hibbert, A. 1975, Comput. Phys. Commun., 9, 141
Pelan, J., & Berrington, K. A. 1995, A&AS, 110, 209
Ramsbottom, C. A., Bell, K. L., & Stafford, R. P. 1996, At. Data Nucl. Data Tables, 63, 57
Ramsbottom, C. A., Berrington, K. A., & Bell, K. L. 1995, At. Data Nucl. Data Tables, 61, 105
Ramsbottom, C. A., Berrington, K. A., Hibbert, A., & Bell, K. L. 1994, Phys. Scr., 50, 246
Saraph, H. E. 1978, Comput. Phys. Commun., 15, 247
Träbert, E. 1993, Phys. Scr., 48, 699